eNeuro

Research Article: New Research | Disorders of the Nervous System

Vascularization and engraftment of transplanted human cerebral organoids in mouse cortex

Nicolas Daviaud[1], Roland H. Friedel[1,2] and Hongyan Zou[1,2]

[1]*Fishberg Department of Neuroscience and Friedman Brain Institute*
[2]*Department of Neurosurgery, Icahn School of Medicine at Mount Sinai, New York, NY 10029, USA*

https://doi.org/10.1523/ENEURO.0219-18.2018

Received: 1 June 2018

Revised: 13 October 2018

Accepted: 27 October 2018

Published: 12 November 2018

Author Contributions: ND: Designed studies, performed experiments, analyzed data, co-wrote the paper. RF and HZ: Designed studies, analyzed data, and co-wrote the paper.

Funding: NIH/NINDS
R01/R56 NS073596

The authors declare no competing financial interests.

Correspondence should be addressed to: Hongyan Zou, Department of Neuroscience, Icahn School of Medicine at Mount Sinai, 1425 Madison Avenue, NY, NY10029. Email: hongyan.zou@mssm.edu.

Cite as: eNeuro 2018; 10.1523/ENEURO.0219-18.2018

Vascularization and engraftment of transplanted human cerebral organoids in mouse cortex

Nicolas Daviaud [1], Roland H. Friedel [1,2], Hongyan Zou [1,2, #]

[1] Fishberg Department of Neuroscience and Friedman Brain Institute,

[2] Department of Neurosurgery, Icahn School of Medicine at Mount Sinai, New York, NY 10029

Abbreviated Title: Cerebral organoid transplant in mice cortex

Author Contributions:

ND: Designed studies, performed experiments, analyzed data, co-wrote the paper. RF and HZ: Designed studies, analyzed data, and co-wrote the paper.

Correspondence should be addressed to:

Hongyan Zou**,** Department of Neuroscience, Icahn School of Medicine at Mount Sinai, 1425 Madison Avenue, NY, NY10029

Email: hongyan.zou@mssm.edu

Key Words

Neural stem cell transplant, cerebral organoid, organoid transplant, vascularization of intracerebral graft

Number of Figures: 9

Number of Tables: 1

Number of Multimedia: 0

Number of words for Abstract: 151

Number of words for Significance Statement: 85

Number of words for Introduction: 819

Number of words for Discussion: 1376

Acknowledgements:

We thank members of Zou and Friedel laboratories for discussions. We thank Didier Trono (EPFL Lausanne) and Linzhao Cheng (Johns Hopkins University) for depositing plasmids to Addgene that were used in this study. We would also like to thank Clement Chevalier and Yoan Fourcade for their helpful discussions about image analysis and statistical analysis, respectively.

Conflict of Interest

The authors declare no competing financial interests

Funding sources

This work was supported by the grants from the National Institutes of Health (R01 NS073596) and Friedman Brain Institute at Icahn School of Medicine at Mount Sinai to H.Z.

Abstract

Neural stem cells hold great promise for neural repair in cases of CNS injury and neurodegeneration, however, conventional cell-based transplant methods face the challenges of poor survival and inadequate neuronal differentiation. Here, we report an alternative, tissue-based transplantation strategy whereby cerebral organoids derived from human pluripotent stem cells were grafted into lesioned mouse cortex. Cerebral organoid transplants exhibited enhanced survival and robust vascularization from host brain as compared to transplants of dissociated neural progenitor cells. Engrafted cerebral organoids harbored a large neural stem cell pool and displayed multilineage neurodifferentiation at two and four week post-grafting. Cerebral organoids therefore represent a promising alternative source to neural stem cells or fetal tissues for transplantation, as they contain a large set of neuroprogenitors and differentiated neurons in a structured organization. Engrafted cerebral organoids may also offer a unique experimental paradigm for modeling human neurodevelopment and CNS diseases in the context of vascularized cortical tissue.

Significance Statement

Neural stem cells hold great promise for neural repair, but conventional cell-based transplant methods face the hurdles of poor graft survival and inadequate neural differentiation. Here, we transplanted cerebral organoids derived from human pluripotent cells into lesioned mouse cortex. We report enhanced survival, robust vascularization, and multilineage differentiation of engrafted human cerebral organoids in host mouse brain. Cerebral organoid transplantation therefore represents an alternative, tissue-based transplantation strategy for neural repair and for modeling human neurodevelopment and CNS diseases in the context of vascularized cortical tissue.

Introduction

Central nervous system (CNS) injury or degeneration results in devastating neurological deficits from irreversible loss of neurons. Functional compensation from surviving neural networks and reparative efforts from endogenous neural stem cells (NSC) are limited in their efficacy. Cell replacement therapy has thus been explored for reconstruction of neural circuits since the early 1970s (Das and Altman, 1972), and the interest has been reignited with the advent of induced pluripotent stem cells (iPSCs) (Takahashi and Yamanaka, 2006) and improved neuronal differentiation protocols (Grade and Götz, 2017; Thompson and Björklund, 2015). Grafted NSC can undergo neuronal and glial differentiation, and display neurite outgrowth (Snyder et al., 1997). However, engraftment rate, long-term survival, and neuronal differentiation remain limited. Hence, novel strategies are needed to advance cell replacement therapy as a viable treatment option for CNS injury or degeneration.

Contrary to the poor engraftment rate of implanted dissociated neural progenitor cells (NPC), mouse embryonic cortical tissue transplants survive well and show successful integration in adult mouse brain with establishment of substantial connectivity with host targets (Gaillard et al., 2007). The proof-of-principle that neural tissue replacement can work in human has been provided by the success of intra-striatal transplantation of human fetal mesencephalic tissue for Parkinson's disease (PD) patients (Kordower et al., 1995). Clinical trials have since been carried out for fetal tissue transplant in PD patients, demonstrating long-term safety and clinical benefits (Barker et al., 2013; Lazic and Barker, 2003). Therefore, a shift from cell-based to tissue-based transplantation represents a promising strategy, but the scarcity of fetal tissues and ethical concerns limit the development of such an approach (Lindvall et al., 2004).

Recently, a novel three dimensional (3D) culture method has been developed to differentiate human pluripotent stem cells (PSC) into cerebral organoids (Lancaster et al., 2013; Lancaster and Knoblich,

2014). Cerebral organoid culture taps into the enormous self-organizing capacity of embryonic stem cells/induced PSC (ESC/iPSC) to form complex tissue structures under defined feeder cell-free conditions, with no addition of exogenous patterning cues or morphogens, an important safety point for transplantation. After 30-day culture in matrigel droplets under rotary condition, cerebral organoids adopt a predominantly dorsal forebrain regional specification, containing fluid-filled ventricle-like structures that are aligned with Sox2+ neuroprogenitors in a ventricular/subventricular-like zone (VZ/SVZ) and Doublecortin (DCX)+ neuroblasts in an outer layer. Rudimentary cortical stratification takes place after longer culture periods, with cortical neurons differentiating into pyramidal identities displaying glutamatergic receptor activity and efferent long-range axons in a stereotypical inside-out stratified layout (Lancaster et al., 2013; Lancaster and Knoblich, 2014). Cerebral organoids thus provide a new experimental platform to study human brain development and to model CNS disorders such as microcephaly (Lancaster et al., 2013; Li et al., 2017), autism spectrum disorders (Forsberg et al., 2018) and Zika virus infection (Qian et al., 2016; Watanabe et al., 2017).

We hypothesized that transplantation of cerebral organoids derived from human ESC/iPSC may enhance graft survival, neural differentiation, and integration in host brain as compared to conventional cell-based transplantation for the following reasons: First, the 3D cellular arrangement of the cortical plate-like tissue in cerebral organoids may provide a protective shield against hostile elements at the graft site. Second, a neuroprecursor pool in the cerebral organoids residing in protected stem cell niches in the VZ/SVZ may serve as a source for neurogenesis and stem cell-derived trophic factors. Third, a rudimentary 3D cortical structure is already in place at the time of transplant, enabling intrinsic patterning cues to direct organized neuronal differentiation and prevent aberrant proliferation and lineage progression.

Here, we performed comprehensive side-by-side comparisons of transplantation of dissociated NPC vs. cerebral organoids, both derived from identical hESC cultures. Postnatal day 8-10 (P8-10) mice were used as recipients and frontoparietal cortex as transplant site. We compared graft survival, vascularization, neural stem cell population, and neurodifferentiation at 2 and 4 weeks after transplantation. We found enhanced survival of cerebral organoid transplants as compared to grafted NPC, and robust vascularization of the organoid grafts from host vessels. There were also abundant neuroprogenitors and evidence for multilineage differentiation in the engrafted cerebral organoids. A recent study by Mansour et. al. also tested intracerebral grafting of hPSC-derived brain organoids (Mansour et al., 2018). In that study, adult NOD-SCID (nonobese diabetic-severe combined immunodeficient) mice were used as recipients and retrosplenial cortex was selected as transplant site based on the rich vascularized surface overlaying this area. They reported that organoid grafts showed successful engraftment with robust vascularization from host brain, and in long-term analysis of up to 8 month post-transplant, progressive neuronal differentiation and maturation, long-range axon projections, and functional graft-to-host synaptic connectivity were observed. Our data thus echo those of Mansour et. al. in demonstrating the practicality of transplantation of hiPSC-derived cerebral organoids as a promising alternative for cell replacement therapy for CNS injury and neurodegeneration. Transplantation of cerebral organoids also provides a unique experimental paradigm to study human neurodevelopment and to model CNS diseases in the context of vascularized cortical tissue.

Material and Methods

Animal Care

Postnatal day 8-10 (P8-10) CD1 mice of either sex (Charles River Laboratories) were used as transplant recipients for analysis up to 4 week post-grafting without immunosuppressive treatment, as immunosuppression was only mandatory to achieve engraftment beyond 2 months (Espuny-Camacho et al., 2013). Mice were group-housed and kept in a 12/12-hour light/ dark cycle with free access to food and water ad libitum. All animal procedures were performed in accordance with the [Author University] animal care committee's regulations.

hESC culture

Human pluripotent embryonic stem cells were provided by WiCell (H9 hES cells, WAe009-A). For hESC culture, 6 well-plates were coated with diluted Matrigel (growth factor reduced) (1:100, BD Biosciences) for 20 min at 37°C, and cells were plated and cultured in mTeSR1 media (STEMCELL Technologies) supplemented with 2 µM ROCK inhibitor Thiazovivin (Millipore) for 24 hr. Cells were cultured with media changed every day until ready to passage or harvest in mTESR1 media (without ROCK inhibitor).

GFP labeling of hESCs

H9 hES cells were infected with lentivirus EF1a-GFP-IRES-Puro, followed by puromycin selection (1 µg/ml, Thermo Fisher Scientific). For lentivirus preparation, the pEGIP lentivirus plasmid (Addgene plasmid #26777) was transfected into 293T cells together with envelope plasmid pMD2.G and packaging plasmid psPAX2 (Addgene #12259 and #12260) with X-tremeGENE 9 DNA transfection reagent (Roche). Lentiviruses were concentrated from culture media supernatant 72 hours after transfection by ultracentrifugation.

Generation of hNPC from hESCs

hES cells were cultured in low attachment 96-well plates for 4 days to generate embryoid bodies (EBs). EBs were then transferred to matrigel-coated 6-well plates for attachment and further cultured in neural induction medium (STEMdiff, STEMCELL Technologies) for 4-5 days. Next, cells were plated on laminin-coated (10 µg/ml, ThermoFisher Scientific) 6-well plates and cultured in human neural stem cell medium (NeuroCult, STEMCELL Technologies) supplemented with 20 ng/ml of epidermal growth factor (EGF) and 10 ng/ml of basic fibroblast growth factor (bFGF) (Peprotech) for 7 days for NPC maturation, which were then used for transplant.

For proliferation and differentiation assays, 12 mm glass coverslips were pre-coated with 50 µg/ml poly-D-lysine (PDL, Sigma Aldrich) and 10 µg/ml laminin (ThermoFisher Scientific). NPC were seeded on coverslips at 12,000 cells/cm^2 density and cultured in human neural stem cell medium (NeuroCult, STEMCELL Technologies) supplemented with 20 ng/ml of EGF and 10 ng/ml of bFGF (Peprotech). For differentiation assays, cells were cultured in the same media, but with withdrawal of mitogens (EGF, bFGF) for 5 days. Cells were fixed with 4% paraformaldehyde (pH 7.4, Acros Organics) in PBS at 4°C for 15 min and analyzed by immunofluorescence.

Cerebral organoid generation from hESCs

Human cerebral organoids were generated as described (Lancaster et al., 2013; Lancaster and Knoblich, 2014), with modifications as follows: Human ES cells were detached using 50 µM EDTA (Thermo Fisher Scientific) and plated in round bottom ultra-low attachment 96-wells plate (CLS7007, Corning) at a density of 9,000 cells per well in mTESR1 media (STEMCELL Technologies) supplemented with 1% antibiotics (Penicillin Streptomycin, ThermoFisher Scientific) for a total of 6 days. During the first 4 days of the culture, media was supplemented with 10 µM of Thiazovivin. Half of the media was changed every day. After 6 days of culture or when embryonic bodies (EBs) reached ~500-600 µm in diameter and when surface tissue began to brighten and formed smooth edges, media was switched to a neural induction media (Stemdiff, STEMCELL Technologies). Half of the media was changed every day for 3-4 days. After neuroepithelium emerged (usually at ~ day 9-10), organoids were

193 embedded in Matrigel droplets (25 µl, BD Biosciences) and cultured in 6 cm Petri dishes (Falcon) for 4
194 days in cerebral organoid differentiation media consisting of 1:1 DMEM-F12 and Neurobasal media
195 (Gibco), with addition of 0.5% N2 supplement (Life Technologies), 0.5% ml MEM-NEAA (Gibco), 1%
196 Glutamax (Gibco), 1% B27 supplement without Vitamin A (Life Technologies), 0.1 µM of 2-
197 Mercaptoethanol (Millipore), 2.6 µg/ml Insulin (Sigma Aldrich), and 1% Pen/Strep antibiotics (Gibco).
198 After 4 days, the organoid Matrigel droplets were cultured with addition of vitamin A on an orbital shaker
199 (VWR) at 85 rpm for 4 additional weeks, and then used for transplant.
200
201 **Grafting of NPC or cerebral organoid into mouse cortex**
202 Before transplantation, a quality control of cerebral organoids was performed by brightfield microscopy
203 to select the organoids that displayed an appropriate differentiation/maturation phenotype without
204 massive cyst formation or premature differentiation. Then, a measurement of organoid size was
205 performed by brightfield microscopy and organoids of similar sizes were selected for transplant. To
206 estimate the cell numbers in organoids at time of transplant, organoids were dissociated by 15 min
207 trypsin incubation, and cells were counted by trypan blue exclusion.
208
209 P8-10 mice were anesthetized with isoflurane and secured on a stereotactic frame (Stoelting). Scalp
210 was opened on the left hemisphere. Using a restricted depth stab knife, an approximately 1 mm x 1 mm
211 craniotomy window was opened, with the bone flap hinged on anterior base. A cortical lesion was made
212 by removing ~1 mm^3 piece of the frontoparietal cortex. Using a pair of forceps, one cerebral organoid
213 at 42-day in vitro culture was implanted into the lesioned mouse cortex. The craniotomy window was
214 closed by returning the bone flap to the original position and sealed with fibrin glue (Evicel, Fibrin
215 Sealant), followed by skin closure with sutures.
216
217 **Intracerebral implantation of NPC**
218 NPC differentiated from H9 hES cells were dissociated with trypsin, counted, and assessed for viability
219 by trypan blue exclusion. Cells were washed twice with DMEM, and then suspended in DMEM at a

concentration of 5 × 10^4/ µl. Using a 5 µl Hamilton syringe (Hamilton glass syringe 600 series RN) and a 26-gauge needle, 1 × 10^5 NPC (2 µl) were implanted into the left frontoparietal hemisphere. To be consistent with the organoid transplant location, the coordinates used for the intracerebral injection were 1 mm posterior to the bregma, 1 mm lateral to the sagittal suture (left hemisphere), and 1 mm below the dura.

Histological analyses

Two or four weeks after transplantation, animals received a lethal dose of pentobarbital (390 mg/ml) and transcardial perfusion was performed with 50 ml cold PBS, followed by 50 ml cold 4% PFA/PBS. Brains were removed and post-fixed overnight in 4% PFA/PBS and cryoprotected for 48 hours in 30% sucrose. Brains were then snapped freeze in isopentane (Sigma Aldrich) and embedded in O.C.T. compound (Tissue-plus, Fisher Healthcare) and stored at -80°C. Brain tissues were sectioned into 14 µm coronal sections with cryostat (CM1850, Leica). For immunofluorescence analysis, non-specific binding sites were blocked with 4% BSA in PBS (Fisher Bioreagents), 0.2% Tween (Tween 20, Acros Organics) and 10% normal donkey serum (Jackson Immunoresearch) for 1 hour at RT, and slices were then incubated with the following antibodies diluted in 4% BSA/PBS, 0.2% Tween: rabbit anti-activated Caspase 3 (Abcam, ab2302, 1:100); rat anti-mouse CD31 (BD Biosciences, 553370, 1:200); rat anti-mouse CD45 (BD Biosciences, 550539, 1:200); guinea pig anti-DCX (Millipore AB2253, 1:500); mouse anti-GalC (Millipore MAB342, 1:200); rabbit anti-GFAP (Invitrogen 180063, 1:200); chicken anti-GFP (Aves Lab, GFP-1020, 1:300); rabbit anti-Iba1 (Wako Chemicals, 019-19741, 1:200); rabbit anti-Ki67 (Abcam, ab15580, 1:500); mouse anti-MTCO2 (Mitochondrially Encoded Cytochrome C Oxidase II) (Abcam, ab110258, 1:100); rabbit anti-Nanog (Abcam, ab109250, 1:300); chicken anti-Neurofilament H (NF-H, Abcam Ab5539, 1:300); mouse anti-Oct4 (Abcam, ab184665, 1:300); rabbit anti-Olig2 (Millipore AB9610, 1:500); rabbit anti-SOX2 (Millipore AB5603, 1:200), rabbit anti-TBR1 (Abcam ab31940, 1:500); rabbit anti-TBR2 (Abcam ab23345, 1:500), mouse anti-tubulin β-III (Tuj1, R&D systems MAB1195, 1:100). Slides were then washed in PBS with 0.1% Tween and detection was

performed with Alexa-coupled secondary antibodies (Invitrogen and Jackson ImmunoResearch) and DAPI nuclear counterstain (Invitrogen).

Quantifications were performed on at least two brain slices per animal and three independent mice for each condition. The two slices were separated by about 150 µm. We selected the sections that were in the middle of the transplant area. Grafts were outlined by GFP or hMito (human mitochondria marker) immunofluorescence. For each selected 14 µm graft-bearing brain slice, we quantified different markers within the entire GFP or hMito-labeled area by Fiji software (Schindelin et al., 2012) unless otherwise specified.

Statistical analysis

For each experiment, the number of mice used in each cohort, and the number of images analyzed from each animal are listed in figure legends. Data are presented as mean value with standard error of the mean (SEM), unless otherwise stated. At least three independent grafts in three different animals were tested and at least two representative images from each animal were quantified.

Cluster-based summary statistics using within-subject averaging were performed whenever possible. GraphPad Prism 7 was used for statistical analyses. Differences between conditions were determined using a two-way analysis of variance (ANOVA) test, followed by a Tukey post hoc test. For individual comparison within the group, normality of data was assessed using a Shapiro–Wilk test followed by a Student T-test. Results were considered significant for p-values <0.05 (Table 1).

Results

hESC-derived NPC and cerebral organoids for intracerebral transplantation

For side-by-side comparisons, we differentiated the same batch of hESC into either NPC or cerebral organoids and performed stereotactic transplantation into left frontoparietal cortex of immunocompetent postnatal day 8-10 (P8-10) mice (Figure 1A). We compared graft survival, vascularization, neural stem cell pool, and neurodifferentiation at 2 and 4 week post-transplantatation (Figure 1B). To ensure that the organoid grafts remained inside the lesion cavity following transplantation, we optimized the technique of opening a small craniotomy window with a bone flap hinged at the anterior base, and after transplantation, the bone flap was returned to original position, sealed with fibrin glue, followed by scalp closure (Figure 1C).

To facilitate visualization of donor cells in host cortical tissue, we generated a human ESC line expressing green fluorescence protein (GFP) ubiquitously (Zou et al., 2009) (Figure 2A). After lentiviral infection and puromycin selection, GFP-expression of hESC was assessed, while their pluripotency was verified by immunocytochemistry with uniform expression of stemness markers Oct4 and Nanog (Figure 2B). GFP-positive hESC were then differentiated into hNPC by way of embryoid body (EB) formation followed by neural induction (Figures 2C, D). To confirm multipotency of hNPC, differentiation condition was applied for 5 days by mitogen withdrawal, and immunocytochemistry revealed expression of TUJ1 (neuronal marker), GFAP (astrocyte marker), and GalC (oligodendrocyte marker) while most cells remained proliferative as shown by the proliferation marker Ki67 (Figure 2E). In parallel, the same batch of GFP-expressing hESC were used to generate cerebral organoids (Lancaster et al., 2013; Lancaster and Knoblich, 2014). GFP expression was confirmed at each stage of organoid development (Figures 2F, G). After 42 days of in vitro culture, with the last 28 days under rotary condition embedded in matrigel droplet, cerebral organoids adopted a predominantly dorsal forebrain specification,

294 containing multiple ventricle-like structures aligned with SOX2+ neuroprogenitors in the VZ/SVZ zone
295 and DCX+ neuroblasts in the outer layer (Figure 2H).

296

297 **Enhanced survival of cerebral organoid transplants**

298 We grafted one single hESC-derived cerebral organoid into the lesion cavity in the left frontoparietal
299 cortex of P8-10 CD1 mice. We determined that the transplanted organoids were composed of an
300 average of 2.5 x 10^5 cells (± 1.4 x 10^5 SEM), with around 22% of cells being Sox2+ neuroprogenitors
301 residing in VZ/SVZ-like structures and the rest of the cells in various stages of neurodifferentiation. In
302 parallel, 1x10^5 dissociated hNPC were implanted into identical cortical location by stereotactic injection,
303 so that comparable number of neuroprogenitors were transplanted in both graft types. At 2 and 4 week
304 post-transplantation, all recipient mice survived the procedure and the transplanted organoids or NPC
305 could be found in each host mouse.

306

307 To compare engraftment rate, we first measured the size of the graft areas as demarcated by GFP-
308 labeled grafted cells. Consistent with earlier reports of poor survival of transplanted NSC in dissociated
309 state (Johann et al., 2007), NPC grafts displayed significant shrinkage from 2 to 4 week time periods
310 post-transplant ($p=0.039$), whereas the size of cerebral organoid grafts remained stable between 2 and
311 4 week post-transplantation (Figures 3A, B). In some instances, organoids grafts appeared fragmented,
312 likely a result of technical difficulty (transplanting a relatively large human cerebral organoid into a small
313 host mouse brain) or cell death from trauma, hypoxia, and inflammation before engraftment took place.
314 Taken together, our finding of an enhanced survival of organoid grafts supports the hypothesis that
315 structured cellular arrangement in tissue-based transplants provides better protection of donor cells
316 from the hostile graft microenvironment.

317

We next examined the extent of apoptosis in NPC vs. organoid transplants by immunohistochemistry for activated caspase 3 (AC3). We found no significant differences in the average number of AC3+ cells per unit GFP+ graft area between the two graft types at 2 week ($p=0.18$) or 4 week ($p=0.96$) post-transplantation, although there were high variabilities (Figures 3C, D). Notably, similar to the finding by Mansour et. al., the number of apoptotic cells were much lower in organoid grafts than in stage-matched cultured organoids (Figure 3E), which may reflect phagocytic clearing in vivo.

To better understand the time course of organoid engraftment, we performed additional short-term post-grafting analyses. We found that by 3 or 5 days after transplantation, organoid grafts had not yet been firmly integrated into host brain tissue as only about 50% of the grafts were found in host animals after tissue processing, indicating insufficient time for engraftment (Figure 3F).

We further examined host immune response against the grafts by immunohistochemistry for Iba1, a marker of activated microglia/macrophages. We detected low number of Iba1+ cells in both NPC and organoid transplants after 2 weeks; but after 4 weeks, the Iba1+ cells were increased and exhibited hypertrophied morphology in NPC transplants and adjacent host brain tissues, suggesting enhanced phagocytic activity. In contrast, Iba1+ cells remained relatively scant and small in size in organoid transplants after 4 weeks (Figure 4A). The Iba1+ cells in the organoid grafts did not co-localize with hMito (human mitochondria marker), indicating host origin of the microglia within the grafts, similar to the data shown by Mansour et. al.. Similar results were observed using leukocyte common antigen CD45. At the transplant sites, we detected only scant $CD45^{hi}$ cells in organoid grafts, and slightly more $CD45^{hi}$ cells in NPC grafts, possibly indicating increased phagocytosis of dead donor cells within the NPC transplants (high regional variability precluded accurate quantification) (Figure 4B).

342 **Successful vascularization from host into the grafted cerebral organoids**

343 Vascularization of the graft is a key determinant for successful integration into host tissue. We therefore
344 compared the extent of graft vascularization by immunohistochemistry for CD31/PECAM1, an
345 endothelial cell marker. We first quantified the number of blood vessels in the entire graft area as labeled
346 by hMito immunostaining. We detected robust vascularization of the organoid transplants at both 2 and
347 4 week post-grafting (Figure 5A). Remarkably, CD31+ microvasculatures were present not only at the
348 periphery, but also at the center of the grafts. Closer inspection revealed no apparent overlap between
349 CD31 and hMito immunostaining, indicating host origin of the graft vasculature. From 2 to 4 weeks
350 following transplantation, the number of microvasculatures in the engrafted organoids remained stable
351 (Figure 5B). In the NPC transplants, we also observed abundant CD31+ microvasculatures within the
352 graft after 2 weeks; but after 4 weeks, a lower number of CD31+ blood vessels were detected (Figure
353 5A). Quantification confirmed the presence of significantly more CD31+ vessels in organoid transplants
354 than in NPC transplants at 4 week post-grafting ($p=0.029$). To verify that the higher number of blood
355 vessels found in organoid transplants was not due to shorter or more branched vasculatures, we
356 measured average vascular length, which was comparable between the two graft types (Figure 5B).
357 Notably, donor cells appeared disorganized in relation to vasculatures in NPC grafts, which may reflect
358 their dissociated state at the time of transplant as compared to the tissue-like cellular arrangement in
359 organoid transplants.

360

361 **Neuroprogenitor proliferation and neurodifferentiation in engrafted cerebral organoids**

362 We next examined proliferation of donor cells in the transplants using the proliferation marker Ki67. A
363 significantly lower density of Ki67+ cells per unit GFP+ graft area was detected in NPC transplants as
364 compared to organoid transplants at both 2 and 4 week post-grafting ($p=0.0014$ and $p=0.0108$,
365 respectively), while there was no significant difference in organoid transplants between the two time
366 points ($p=0.97$) (Figure 6A, B). The percent of Ki67+/DAPI+ cells at 2 week post-transplantation was

also much lower in NPC transplants (~2.5%) than in organoid transplants (~9%) (p=0.038), but the difference at 4 week became more variable, thus not statistically significant (~4.5% in NPC grafts and 9% in organoid grafts, p=0.21) (Figure 6B). Of note, in NPC cultures, proliferative cells were abundant, even after 5 days under differentiation condition (shown in Fig. 2E); in contrast, in cultured organoids, Ki67+ cells were restricted to VZ/SVZ (Fig. 2H). Therefore, the starting number of proliferative cells in NPC transplants may in fact be higher than in organoids transplants. There was no significant difference in the percent of Ki67+/DAPI+ cells in the organoid grafts between 2 and 4 week post-grafting (p=0.99). It is also notably that unlike in stage-matched cultured organoids where Ki67+ proliferative cells were detected predominantly in the progenitor zones aligning the ventricle-like structures (Figure 7A), the Ki67+ cells in transplanted organoids appeared scattered throughout the grafts, reflecting disintegration of the ventricular structures following transplantation.

We also assessed neuroprogenitor populations in the two graft types. The Sox2+ neuroprogenitors remained abundant in both graft types, with comparable density at 2 and 4 week post-transplantation. In regards to the percent of Sox2+/DAPI+ cells, the results were also comparable for NPC and organoid transplants with ~30% cells expressing Sox2 at both time points (Figure 6C, D). However, as the surviving NPC grafts markedly shrunk in size from 2 to 4 week post-grafting, the total number of Sox2+ neuroprogenitors in the NPC grafts became markedly smaller; in contrast, there was a stable and sizable neural stem cell pool in the organoid transplants at both time points (Figure 6C). Similar to the Ki67 results, the Sox2+ cells also became scattered in the grafts, unlike in stage-matched cultured cerebral organoids where Sox2+ cells resided in the VZ/SVZ aligning ventricle-like structures (Figure 7A). It is also worth mentioning that the host cortex also contains numerous Sox2+ oligodendrocyte precursor cells (OPC).

We next compared neurodifferentiation in the two graft types. We detected significantly more DCX+ neuroblasts per unit area of GFP+ organoid transplants than NPC transplants at 4 week post-transplantation ($p=0.03$) (Figure 8A, B). This indicates enhanced survival and neuronal differentiation in the engrafted organoids. Temporal analysis showed comparable numbers of DCX+ neuroblasts within the organoid transplants at 2 and 4 weeks after grafting ($p=0.17$). The DCX+ cells did not seem to follow any particular pattern in relationship to ventricular proximity in host brains. Astrocyte differentiation also appeared significantly more prominent in organoid transplants than in NPC grafts at 4 week post-transplantation ($p=0.0006$), although at 2 week, the expression levels of GFAP per unit graft area were comparable between the two graft types (Figure 8C, D). Temporal comparison showed a significant increase of GFAP expression within organoid transplants between 2 and 4 week post-grafting ($p=0.004$). It is worth noting the central location of GFAP+ cells within the grafts and the co-localization of GFAP and hMito immunofluorescence, which support donor origin of the astrocytes (as opposed to infiltrating host reactive astrocytes). Finally, the presence of the oligodendrocyte lineage was examined by Olig2 immunofluorescence. We observed an average of 10.8% and 12.4% of cells expressing Olig2 in organoid grafts at 2 and 4 week post-transplantation, respectively (Figure 8E, F). In stage-matched cultured cerebral organoids, there were abundant DCX+ neuroblasts in organoids at both 6 and 8 weeks of culture, scant GFAP+ astrocytes at 8 weeks of rotary culture, but no detectable Olig2+ cells at either 6 or 8 weeks (Figure 7B).

Further characterization of neuronal differentiation in the engrafted cerebral organoids showed the presence of cells expressing TBR2 (also known as EOMES), a marker for intermediate progenitor cells (Englund et al., 2005), which appeared more abundant at 2 weeks as compared to 4 weeks after grafting (Figure 9A). Notably, there were no TBR2-expressing cells in the host cortex. We also observed cells expressing CTIP2, a marker corresponding to deep layer neurons, particularly at 4 week post-grafting (Figure 9B). These data are in agreement with the temporal pattern of lineage progression of neuronal

differentiation, however, no layer organizations of CTIP2-positive neurons were detected in the organoid transplants, unlike in stage-matched cerebral organoid cultures (Figure 7A).

To further assess the presence of mature neurons in different transplants and examine axonal growth and projections, we performed immunostaining for the neurofilament heavy chain (NF-H). While no NF-H immunosignals were detected at 2 or 4 weeks after NPC transplantation (data no shown), there was co-localization of NF-H and hMito immunosignals in organoid transplants at both time-points, some with long projections (Figure 9C). However, no organized projection pattern was detected, which may reflect the short time frame of the current experimental paradigm. In stage-matched cerebral organoid cultures, we also detected only low NF-H+ immunosignals (Figure 7B).

Discussion

In conventional stem cell transplantation approaches, dissociated stem cells are deposited in suspension through intra-cerebral, -venous, -arterial, or transnasal routes, all of which expose the transplanted cells to immediate hostile elements in the host brain, resulting in poor survival (Bliss et al., 2007; Chen et al., 2011). Here, we conducted side-by-side comparison of transplanting human cerebral organoids vs. dissociated human NPC that were derived from the same batch of hESCs and into identical cortical locations. We demonstrated enhanced survival of organoid grafts as compared to NPC transplants, thus supporting the notion that grafting donor cells in tissue-like cerebral organoids with 3D cytoarchitecture is an essential step to enhance graft viability by providing a protective shield against hostile host elements.

It is noteworthy of the technically challenges of the current study, which entails creating a large cavity in a small host mouse brain and grafting a relatively large human cerebral organoid; in comparison, stereotactic injection of dissociated stem cells is less traumatic. The use of adult mice as recipients may ease some of the technical difficulties, and a recent study successfully demonstrated intracranial transplant of human cerebral organoids into adult mice brains (Mansour et al., 2018). However, the different study design of the two studies and the different time frame of post-transplant analyses warrant careful comparison regarding the potential influences of transplant location, the age of the host mice, SCID vs. immunocompetent recipient mice on the survival and development of organoid grafts. Despite these differences, many similar findings emerge from the two studies that echo each other: First, both studies found extensive vascularization from host brain into organoid grafts by 14 days after transplantation. Second, engraftment speed and expansion of the organoid grafts appeared comparable in both studies with overall reduction in graft size from day 0 to day 14 before vascularization takes place. Third, in both studies, human organoid grafts contained Iba1+ microglia that were of host origin. Four, both studies found limited programmed cell death in the organoid grafts in contrast to the massive apoptosis seen in stage-matched organoids in culture, which may be a result of robust vascularization and in vivo phagocytic clearing. Fifth, the time frames of neuronal and glial differentiation in engrafted cerebral organoids were similar in both studies, with scant axonal processes and low number of astrocyte differentiation by 14 days, which then increased in abundance over time.

A good vascularization is key for survival and development of grafted tissue (Bates et al., 2016; Casper et al., 2003; Péron et al., 2017). Remarkably, 2 weeks after transplantation, both NPC and organoid transplants have already attracted robust penetration of host vessels into the grafts, suggesting abundant vascular growth factors released from neuroprogenitors in the grafts. It also indicates that the poor survival of NPC transplants after 4 weeks cannot be simply explained by lack of vascularization. One major difference between the two graft types is a much more organized cellular arrangement and

463 tissue-like cytoarchitecture in organoid transplants, in contrast to the random organization and
464 dissociated state of donor cells in NPC transplants. Indeed, earlier studies showed that transplantation
465 of tissue pieces results in better survival compared to cell suspension grafts (Clarkson et al., 1998;
466 Sekine et al., 2011). Three-dimensionality, cell-cell support from multiple cell types, and cell–matrix
467 interaction all help to improve the success of tissue transplants (Tate et al., 2009). Hence, akin to tissue-
468 based transplantation, cerebral organoid transplants likely confer better protection and trophic support
469 for donor cells as a result of proper cytoarchitecture. Furthermore, donor cells in the organoid
470 transplants continue to benefit from exposure to intrinsic patterning cues that are concordant with
471 developmental stages, while the stem cell niches in the progenitor zone of cerebral organoids can
472 provide proper biomechanical properties and spatial cues important for donor cell survival, proliferation,
473 and lineage progression. This is reflected by a steady fraction of proliferative cells and enhanced
474 multilineage neurodifferentiation in the organoid transplants. In addition, as we used P8-10 mice as
475 recipients and relatively large sized organoid transplants, the survival of our organoid grafts may have
476 also benefited from spatial proximity to the lateral ventricles and the retrosplenial cortex with rich
477 vascularized surfaces (Mansour et al., 2018).

478

479 Neural stem cell therapies have been shown to improve functional outcome in a variety of CNS disease
480 models, and the benefits have largely been attributed to trophic support or immunomodulation
481 (Fainstein et al., 2013; Pluchino and Martino, 2008). In cerebral organoid transplants, we detected a
482 sustained neural stem cell pool, which by itself may significantly contribute to tissue repair. It is worth
483 noting that the spatial organization of neuroprogenitors along ventricles in the cerebral organoids was
484 largely lost by day 14 following transplantation, as shown by the scattering patterns of Sox2+ cells and
485 Ki67+ cells throughout the grafts. Regardless, compared to NPC transplanted in suspension, donor
486 neuroprogenitor cells in organoid grafts would still benefit from a microenvironment with three-
487 dimensionality and in vivo-like cytoarchitecture. Regarding neurodifferentiation, there is increased
488 progeny cells of neuronal lineage in the organoid grafts with DCX+ neuroblasts and CTIP+ cortical

neurons. Astrocyte differentiation in the organoid transplants appears increased between 2 and 4 week post-grafting, consistent with the developmental timeline of gliogenesis, which occurs after the main phase of neurogenesis (Ge et al., 2012). The number of GFAP+ cells in organoid grafts appears more abundant than in stage-matched organoid cultures (Figure 7B). This may reflect stronger glial differentiation signals at the transplant site in vivo than in cultured organoids. Concordantly, as compared to in vitro cerebral organoid cultures where oligodendrocytes were detected only at later stages (Matsui et al., 2018; Renner et al., 2017), we detected ~10% donor cells expressing Olig2 at both 2 and 4 week post-grafting. Of note, during human neurodevelopment, Olig2 is expressed in OPC but also in a subset of neuroprogenitors (Jakovcevski and Zecevic, 2005), thus the Olig2+ cells in the organoid grafts may represent both populations.

Organoid transplantations have been examined for different target organs, including lung organoids (Dye et al., 2016), photoreceptor organoids (Santos-Ferreira et al., 2016), and liver organoids (Nie et al., 2018), all of which demonstrated good engraftment and maturation of transplanted organoids. In the current study, we limited the timeframe of our analyses to 2 and 4 weeks after transplantation, as immunocompetent P8-10 mice were used with no immunosuppressive treatment. To investigate later time-points, SCID mice or immunosuppression will be necessary. Mansour et. al. recently detailed neurodevelopment in transplanted cerebral organoids up to 180 days after transplant, at which time extensive axonal growth and graft-to-host axonal projections, as well as functional synapses were observed (Mansour et al., 2018). In both the current study and the study by Mansour et. al., organoids were grown in culture for 40–50 days from hESCs (~4 weeks in Matrigel rotary condition) with largely dorsal forebrain specification, transplanting organoids of different maturity or of different regional specification by varying culture period or including different morphogen are worthwhile in future studies. Recent advancement allowed generation of region-specific neural organoids with features of neocortex (Lee et al., 2017), telencephalon (Watanabe et al., 2005), cerebellum (Muguruma et al., 2015), neural tube (Ranga et al., 2016), hippocampus (Sakaguchi et al., 2015), and neural retina (Kuwahara et al.,

2015), among others (Wei et al., 2017). These specialized neural organoids open the door for further testing of homotypic transplants wherein region-specific cerebral organoids are transplanted into the corresponding region in host brain. In this regard, an earlier study showed substantially different set of efferent axon projections from transplants of homotypic embryonic motorcortex vs. heterotopic embryonic visual cortical tissue into adult motor cortex (Gaillard et al., 2007). Additional studies are needed to control stem cell proliferation, as iPSC derivatives may have oncogenic potential even after differentiation (Blum and Benvenisty, 2008; Ghosh et al., 2011). Finally, ethical questions need to be discussed concerning the use and further development of more complex cerebral organoids (Lavazza and Massimini, 2018).

In summary, our study demonstrated enhanced survival and robust vascularization of human cerebral organoid transplants in lesioned frontoparietal cortex of mouse hosts. Cerebral organoid transplantations may offer a promising novel cell replacement strategy for repair of CNS injury and neurodegenerative disorders as they provide a large set of neural cell types with both neuroprogenitors and differentiated neurons in a structured organization similar to the targeted brain area.

References

Barker RA, Barrett J, Mason SL, Björklund A (2013) Fetal dopaminergic transplantation trials and the future of neural grafting in Parkinson's disease. Lancet Neurol 12:84–91.

Bates KA, Drummond ES, Cozens GS, Harvey AR (2016) Vascular insufficiency, not inflammation, contributes to chronic gliosis in a rat CNS transplantation model. Restor Neurol Neurosci 34:313–323.

Bliss T, Guzman R, Daadi M, Steinberg GK (2007) Cell transplantation therapy for stroke. Stroke 38:817–826.

Blum B, Benvenisty N (2008) The Tumorigenicity of Human Embryonic Stem Cells In: Advances in Cancer Research , pp133–158.

Casper D, Finkelstein E, Goldstein IM, Palencia D, Yunger Y, Pidel A (2003) Dopaminergic neurons associate with blood vessels in neural transplants. Exp Neurol 184:785–793.

Chen H, Yoshioka H, Kim GS, Jung JE, Okami N, Sakata H, Maier CM, Narasimhan P, Goeders CE, Chan PH (2011) Oxidative stress in ischemic brain damage: mechanisms of cell death and potential molecular targets for neuroprotection. Antioxid Redox Signal 14:1505–1517.

Clarkson ED, Zawada WM, Adams FS, Bell KP, Freed CR (1998) Strands of embryonic mesencephalic tissue show greater dopamine neuron survival and better behavioral improvement than cell suspensions after transplantation in parkinsonian rats. Brain Res 806:60–68.

Das GD, Altman J (1972) Studies on the transplantation of developing neural tissue in the mammalian brain. I. Transplantation of cerebellar slabs into the cerebellum of neonate rats. Brain Res 38:233–49.

555 Dye BR, Dedhia PH, Miller AJ, Nagy MS, White ES, Shea LD, Spence JR (2016) A bioengineered
556 niche promotes in vivo engraftment and maturation of pluripotent stem cell derived human lung
557 organoids. Elife 5.

558 Englund C, Fink A, Lau C, Pham D, Daza RAM, Bulfone A, Kowalczyk T, Hevner RF (2005) Pax6,
559 Tbr2, and Tbr1 Are Expressed Sequentially by Radial Glia, Intermediate Progenitor Cells, and
560 Postmitotic Neurons in Developing Neocortex. J Neurosci 25:247–251.

561 Espuny-Camacho I, Michelsen KA, Gall D, Linaro D, Hasche A, Bonnefont J, Bali C, Orduz D, Bilheu
562 A, Herpoel A, Lambert N, Gaspard N, Peron S, Schiffmann SN, Giugliano M, Gaillard A,
563 Vanderhaeghen P (2013) Pyramidal neurons derived from human pluripotent stem cells integrate
564 efficiently into mouse brain circuits in vivo. Neuron 77:440–456.

565 Fainstein N, Einstein O, Cohen ME, Brill L, Lavon I, Ben-Hur T (2013) Time limited
566 immunomodulatory functions of transplanted neural precursor cells. Glia 61:140–149.

567 Ford AL, Goodsall AL, Hickey WF, Sedgwick JD (1995) Normal adult ramified microglia separated
568 from other central nervous system macrophages by flow cytometric sorting. Phenotypic
569 differences defined and direct ex vivo antigen presentation to myelin basic protein-reactive CD4+
570 T cells compared. J Immunol 154:4309–21.

571 Forsberg SL, Ilieva M, Maria Michel T (2018) Epigenetics and cerebral organoids: promising
572 directions in autism spectrum disorders. Transl Psychiatry 8:14.

573 Gaillard A, Prestoz L, Dumartin B, Cantereau A, Morel F, Roger M, Jaber M (2007) Reestablishment
574 of damaged adult motor pathways by grafted embryonic cortical neurons. Nat Neurosci 10:1294–
575 1299.

576 Ge W-PP, Miyawaki A, Gage FH, Jan YN, Jan LY (2012) Local generation of glia is a major astrocyte
577 source in postnatal cortex. Nature 484:376–380.

578 Ghosh Z, Huang M, Hu S, Wilson KD, Dey D, Wu JC (2011) Dissecting the Oncogenic and
579 Tumorigenic Potential of Differentiated Human Induced Pluripotent Stem Cells and Human
580 Embryonic Stem Cells. Cancer Res 71:5030–5039.

581 Grade S, Götz M (2017) Neuronal replacement therapy: previous achievements and challenges
582 ahead. npj Regen Med 2:29.

583 Jakovcevski I, Zecevic N (2005) Olig Transcription Factors Are Expressed in Oligodendrocyte and
584 Neuronal Cells in Human Fetal CNS. J Neurosci 25:10064–10073.

585 Johann V, Schiefer J, Sass C, Mey J, Brook G, Krüttgen A, Schlangen C, Bernreuther C, Schachner
586 M, Dihné M, Kosinski CM (2007) Time of transplantation and cell preparation determine neural
587 stem cell survival in a mouse model of Huntington's disease. Exp Brain Res 177:458–470.

588 Kordower JH, Freeman TB, Snow BJ, Vingerhoets FJG, Mufson EJ, Sanberg PR, Hauser RA, Smith
589 DA, Nauert GM, Perl DP, Olanow CW (1995) Neuropathological Evidence of Graft Survival and
590 Striatal Reinnervation after the Transplantation of Fetal Mesencephalic Tissue in a Patient with
591 Parkinson's Disease. N Engl J Med 332:1118–1124.

592 Kuwahara A, Ozone C, Nakano T, Saito K, Eiraku M, Sasai Y (2015) Generation of a ciliary margin-
593 like stem cell niche from self-organizing human retinal tissue. Nat Commun 6:6286.

594 Lancaster MA, Knoblich JA (2014) Generation of cerebral organoids from human pluripotent stem
595 cells. Nat Protoc 9:2329–2340.

596 Lancaster MA, Renner M, Martin CA, Wenzel D, Bicknell LS, Hurles ME, Homfray T, Penninger JM,
597 Jackson AP, Knoblich JA (2013) Cerebral organoids model human brain development and
598 microcephaly. Nature 501:373–379.

599 Lavazza A, Massimini M (2018) Cerebral organoids: ethical issues and consciousness assessment. J
600 Med Ethics 0:1–5.

601 Lazic SE, Barker RA (2003) The future of cell-based transplantation therapies for neurodegenerative
602 disorders. J Hematother Stem Cell Res 12:635–642.

603 Lee C-T, Chen J, Kindberg AA, Bendriem RM, Spivak CE, Williams MP, Richie CT, Handreck A,
604 Mallon BS, Lupica CR, Lin D-T, Harvey BK, Mash DC, Freed WJ (2017) CYP3A5 Mediates
605 Effects of Cocaine on Human Neocorticogenesis: Studies using an In Vitro 3D Self-Organized
606 hPSC Model with a Single Cortex-Like Unit. Neuropsychopharmacology 42:774–784.

607 Li R, Sun L, Fang A, Li P, Wu Q, Wang X (2017) Recapitulating cortical development with organoid
608 culture in vitro and modeling abnormal spindle-like (ASPM related primary) microcephaly
609 disease. Protein Cell 8:823–833.

610 Lindvall O, Kokaia Z, Martinez-Serrano A (2004) Stem cell therapy for human neurodegenerative
611 disorders-how to make it work. Nat Med 10 Suppl:S42-50.

612 Mansour AA, Gonçalves JT, Bloyd CW, Li H, Fernandes S, Quang D, Johnston S, Parylak SL, Jin X,
613 Gage FH (2018) An in vivo model of functional and vascularized human brain organoids. Nat
614 Biotechnol 36:432–441.

615 Matsui TK, Matsubayashi M, Sakaguchi YM, Hayashi RK, Zheng C, Sugie K, Hasegawa M,
616 Nakagawa T, Mori E (2018) Six-month cultured cerebral organoids from human ES cells contain
617 matured neural cells. Neurosci Lett 670:75–82.

618 Muguruma K, Nishiyama A, Kawakami H, Hashimoto K, Sasai Y (2015) Self-Organization of Polarized
619 Cerebellar Tissue in 3D Culture of Human Pluripotent Stem Cells. Cell Rep 10:537–550.

620 Nie Y-Z, Zheng Y-W, Ogawa M, Miyagi E, Taniguchi H (2018) Human liver organoids generated with
621 single donor-derived multiple cells rescue mice from acute liver failure. Stem Cell Res Ther 9:5.

622 Péron S, Droguerre M, Debarbieux F, Ballout N, Benoit-Marand M, Francheteau M, Brot S, Rougon
623 G, Jaber M, Gaillard A (2017) A Delay between Motor Cortex Lesions and Neuronal

624 Transplantation Enhances Graft Integration and Improves Repair and Recovery. J Neurosci
625 37:1820–1834.

626 Pluchino S, Martino G (2008) Neural stem cell-mediated immunomodulation: repairing the
627 haemorrhagic brain. Brain 131:604–605.

628 Qian X et al. (2016) Brain-Region-Specific Organoids Using Mini-bioreactors for Modeling ZIKV
629 Exposure. Cell 165:1238–1254.

630 Ranga A, Girgin M, Meinhardt A, Eberle D, Caiazzo M, Tanaka EM, Lutolf MP (2016) Neural tube
631 morphogenesis in synthetic 3D microenvironments. Proc Natl Acad Sci U S A 113:E6831–
632 E6839.

633 Renner M, Lancaster MA, Bian S, Choi H, Ku T, Peer A, Chung K, Knoblich JA (2017) Self-organized
634 developmental patterning and differentiation in cerebral organoids. EMBO J 36:1316–1329.

635 Sakaguchi H, Kadoshima T, Soen M, Narii N, Ishida Y, Ohgushi M, Takahashi J, Eiraku M, Sasai Y
636 (2015) Generation of functional hippocampal neurons from self-organizing human embryonic
637 stem cell-derived dorsomedial telencephalic tissue. Nat Commun 6:8896.

638 Santos-Ferreira T, Völkner M, Borsch O, Haas J, Cimalla P, Vasudevan P, Carmeliet P, Corbeil D,
639 Michalakis S, Koch E, Karl MO, Ader M (2016) Stem Cell–Derived Photoreceptor Transplants
640 Differentially Integrate into Mouse Models of Cone-Rod Dystrophy. Investig Opthalmology Vis Sci
641 57:3509.

642 Schindelin J, Arganda-Carreras I, Frise E, Kaynig V, Longair M, Pietzsch T, Preibisch S, Rueden C,
643 Saalfeld S, Schmid B, Tinevez J-Y, White DJ, Hartenstein V, Eliceiri K, Tomancak P, Cardona A
644 (2012) Fiji: an open-source platform for biological-image analysis. Nat Methods 9:676–682.

645 Sekine H, Shimizu T, Dobashi I, Matsuura K, Hagiwara N, Takahashi M, Kobayashi E, Yamato M,
646 Okano T (2011) Cardiac Cell Sheet Transplantation Improves Damaged Heart Function via

Superior Cell Survival in Comparison with Dissociated Cell Injection. Tissue Eng Part A 17:2973–2980.

Snyder EY, Yoon C, Flax JD, Macklis JD (1997) Multipotent neural precursors can differentiate toward replacement of neurons undergoing targeted apoptotic degeneration in adult mouse neocortex. Proc Natl Acad Sci U S A 94:11663–8.

Takahashi K, Yamanaka S (2006) Induction of Pluripotent Stem Cells from Mouse Embryonic and Adult Fibroblast Cultures by Defined Factors. Cell 126:663–676.

Tate CC, Shear DA, Tate MC, Archer DR, Stein DG, LaPlaca MC (2009) Laminin and fibronectin scaffolds enhance neural stem cell transplantation into the injured brain. J Tissue Eng Regen Med 3:208–217.

Thompson LH, Björklund A (2015) Reconstruction of brain circuitry by neural transplants generated from pluripotent stem cells. Neurobiol Dis 79:28–40.

Watanabe K, Kamiya D, Nishiyama A, Katayama T, Nozaki S, Kawasaki H, Watanabe Y, Mizuseki K, Sasai Y (2005) Directed differentiation of telencephalic precursors from embryonic stem cells. Nat Neurosci 8:288–296.

Watanabe M et al. (2017) Self-Organized Cerebral Organoids with Human-Specific Features Predict Effective Drugs to Combat Zika Virus Infection. Cell Rep 21:517–532.

Wei N, Quan Z, Tang H, Zhu J (2017) Three-Dimensional Organoid System Transplantation Technologies in Future Treatment of Central Nervous System Diseases. Stem Cells Int 2017:1–14.

Zou J, Maeder ML, Mali P, Pruett-Miller SM, Thibodeau-Beganny S, Chou B-K, Chen G, Ye Z, Park I-H, Daley GQ, Porteus MH, Joung JK, Cheng L (2009) Gene Targeting of a Disease-Related Gene in Human Induced Pluripotent Stem and Embryonic Stem Cells. Cell Stem Cell 5:97–110.

Figure Legends

Figure 1. Schematic depiction of intracranial transplantation of human cerebral organoids.

A) hES cells were differentiated into NPC or cerebral organoids. Stereotactic surgery was performed to transplant one single cerebral organoid in the lesioned frontoparietal cortex in postnatal day 8-10 mice. For NPC transplantation, dissociated NPC were implanted into identical cortical region by stereotactic injection.

B) Experimental timeline. P8-10 immunocompetent mice were used as recipients for transplantation of dissociated human NPC or human cerebral organoids. Histological analyses of the grafts were performed 2 or 4 weeks after grafting.

C) Schematic diagrams (top) and intra-operative photos (bottom) of cerebral organoid transplantation. Briefly, from left to right, once scalp is reflected, a small craniotomy window was opened with the bone flap hinged at the anterior base, and a small piece of the frontoparietal cortex (~1 mm^3) was removed. A single cerebral organoid was then implanted into the prelesioned mouse cortex, followed by return of the bone flap to close the craniotomy window, sealed with fibrin glue, followed by scalp closure.

Figure 2. Characterization of GFP-labeled NPC and cerebral organoids derived from hESC.

A) Diagram of lentiviral vector expressing EGFP (enhanced GFP) driven by EF-1a promoter to label hES cells.

B) Phase-contrast and fluorescent images of GFP-labeled hES cells (left) and expression of pluripotency markers Oct4 (green) and Nanog (red) (right).

C) Timeline of differentiation of hES cells into NPC.

D) Phase-contrast and fluorescent images of human NPC derived from GFP-labeled hES cells.

E) Representative immunofluorescence images of NPC stained for proliferation marker Ki67 and the indicated neural markers.

F) Timeline of derivation of cerebral organoids from hESC.

G) Left panels: phase-contrast and fluorescence images of GFP-labeled EB or Matrigel-embedded cerebral organoids. Right panel: immunofluorescent images of sectioned cerebral organoids stained for GFP.

H) Phase-contrast image of cerebral organoid at day 42 of culture and immunofluorescent images of sectioned day 42 cerebral organoid stained for the indicated markers. V: ventricle-like structures. Note the proliferative zone (Ki67+) and Sox2+ neuroprogenitors at the ventricular/subventricular-like zone, and DCX+ neuroblasts in the outer layer.

Figure 3. Engraftment and survival of NPC and cerebral organoid transplants.

A) Representative immunofluorescence images of NPC transplant (left) and cerebral organoid transplant (right) at the indicated time points post-grafting. Enlarged images of the boxed area are shown at the bottom. D: dorsal, V: ventral, M: medial, L: lateral.

B) Quantification showing the relative size of GFP-positive area of NPC and organoid transplants at 2 and 4 week post-grafting. A significant decrease of the graft size of the NPC transplants was detected at 4 week as compared to 2 week post-grafting.

C) Representative immunofluorescence images for hMito (human mitochondria) and activated caspase 3 (AC3) in NPC transplants (left) or in cerebral organoid transplants (right) at the indicated time points after transplantation.

D) Quantification showing the number of AC3-positive apoptotic cells per unit area of hMito-positive grafts at the indicated time points.

E) Representative immunofluorescence images showing a high number of apoptotic cells (AC3+) in stage-matched cerebral organoids in culture at 6 and 8 weeks.

718 F) Representative immunofluorescence images of NPC transplant (left) and cerebral organoid grafts
719 (right) 3 or 5 days after transplantation. At these early time-points, grafts had not yet been firmly
720 integrated into host brains.

721 Dashed white lines delineate the graft areas. *, $p<0.05$. n.s., non-statistically significant. 2-way ANOVA
722 followed by a Tukey post hoc test. n= 3 mice for each time point and two images from each mouse.

723

724 **Figure 4. Host immune response following NPC and organoid transplants.**

725 A) Representative immunofluorescence images of Iba1 in hMito-labeled grafts, at 2 and 4 weeks after
726 transplantation. Note the hypertrophied Iba1+ microglia inside the NPC graft, as well as in host brain
727 tissue adjacent to the NPC graft (white arrowhead).

728 B) Representative immunofluorescence images of CD45 in GFP-labeled grafts at indicated time-points.

729 Dashed white lines delineate the graft areas. Enlarged images of the boxed area are shown on the right.
730 D: dorsal, V: ventral, M: medial, L: lateral.

731

732 **Figure 5. Vascularization of engrafted cerebral organoids.**

733 A) Representative immunofluorescence images demonstrate penetration of host CD31-positive blood
734 vessels into hMito+ NPC grafts (left panels) or cerebral organoid grafts (right panels) at the indicated
735 time points post-transplantation. Notice that CD31-positive endothelial cells inside the grafts are hMito-
736 negative (white arrowheads). White arrows: host vasculature. Dashed white lines delineate the graft
737 areas. Enlarged images of the boxed area are shown on the right. D: dorsal, V: ventral, M: medial, L:
738 lateral.

739 B) Quantifications of the number (left) and the average length (right) of CD31-positive blood vessels in
740 hMito-labeled grafts demonstrate a higher number of vasculatures in the engrafted cerebral organoids

compared to NPC transplants at 4 week post-transplantation, but no significant difference in the average vascular length. *, p<0.05; n.s., non-statistically significant. n= 3 mice for each cohort, and at least two images analyzed from each mouse. 2-way ANOVA followed by a Tukey post hoc test.

Figure 6. Cell proliferation and neural stem cell pool in cerebral organoid transplants.

A) Representative immunofluorescence images of NPC (left panels) and cerebral organoid transplants (right panels) stained for GFP and proliferation marker Ki67. D: dorsal, V: ventral, M: medial, L: lateral.

B) Quantification (top) showing a higher density of Ki67+ cells per unit GFP+ area in cerebral organoid than in NPC transplants at both 2 and 4 week post-transplantation. Bottom quantification: percent of Ki67+ /DAPI+ cells within the GFP+ cerebral organoid and NPC grafts.

C) Representative immunofluorescence images of NPC (left panels) and cerebral organoid transplants (right panels) showing abundant engrafted cells (GFP+) expressing stem cell marker Sox2 (red). White arrows: Sox2+ OPC in host cortical tissue.

D) Quantification (top) showing no significant difference of the density of Sox2+ cells per unit GFP+ area between NPC and cerebral organoid transplants at either time-points. Bottom quantification: percent of Sox2+/DAPI+ cells within the organoid and NPC grafts showing no significant difference between the two types of transplants at either time-point.

Dashed white lines delineate the graft areas. Enlarged images of the boxed area are shown on the right. *, p<0.05; n.s., non-statistically significant. 2-way ANOVA followed by a Tukey *post hoc* test. n= 3 mice for each time point and at least 2 images from each mouse.

Figure 7. Stage-matched in vitro cerebral organoid characterization.

A) Representative immunofluorescence images of cultured cerebral organoids at 6 or 8 weeks of maturation show layered organization of cortical-like tissue with proliferating cells (Ki67+) and NPC (SOX2+) mainly localized in the VZ/SVZ and neurons (CTIP2+) localized in the outer layer.

B) Representative immunofluorescence images of cerebral organoids after 6 or 8 weeks of in vitro maturation. Left: a low number of astrocytes (GFAP+) was present in the organoids after 8 weeks of maturation (white arrow), while no Olig2+ cells were detected. Right: abundant neuroblasts (DCX+) were found at both time-points while low level of expression of NF-H was detected at 8 weeks of maturation.

Figure 8. Neurodifferentiation of the engrafted C-organoids.

A) Representative immunofluorescent images of DCX-positive neuroblasts in NPC (left panels) and cerebral organoid transplants (right panels) at the indicated time points. D: dorsal, V: ventral, M: medial, L: lateral.

B) Quantification of DCX immunointensity per unit area of GFP+ grafts. A significant stronger staining intensity of DCX was measured in organoid compared to NPC transplants after 4 weeks.

C) Representative immunofluorescence images of GFAP+ cells in hMito-labeled NPC (left) and organoids grafts (right) at the indicated time points. White arrows denote colocalization of hMito and GFAP markers in transplants.

D) Quantification of GFAP immunointensity per unit area of hMito+ grafts. A significant stronger staining intensity of GFAP was measured in organoid transplants after 4 weeks.

E) Representative immunofluorescence images of Olig2+ cells in the engrafted cerebral organoids at the indicated time points. White arrows: Olig2+ cells in host cortical tissue.

F) Quantification shows no significant difference in the percent of Olig2+/DAPI+ cells in the organoid grafts between 2 and 4 week post-grafting.

Dashed white lines delineate the graft areas. Enlarged images of the boxed area are shown on the right. *, p<0.05; n.s., non-statistically significant. 2-way ANOVA followed by a Tukey post hoc test and Student t-test. n= 3 mice for each time point and two images from each mouse.

Figure 9. Differentiation of cerebral organoid transplants.

A) Representative immunofluorescence images showing cells expressing intermediate progenitor marker TBR2 in the engrafted cerebral organoids at 2 and 4 week post-transplantation. Notice no TBR2+ cells were observed in host cortical tissue and a slight decline of the number of TBR2+ cells in the hMito+ organoid grafts from 2 to 4 week post-transplantation.

B) Representative immunofluorescence images showing cells expressing deep layer neuronal marker CTIP2 in the engrafted cerebral organoids at 2 and 4 post-transplantation. Notice CTIP2+ cells in neighboring host cortex (white arrows), while in the hMito+ organoid grafts, there was an increase of CTIP2+ cells from 2 to 4 weeks after transplantation.

C) Representative immunofluorescence images show expression of neurofilament heavy (NF-H) in the transplanted organoids after 2 and 4 weeks. White arrowheads denote colocalization of NH-H and hMito in organoid transplants.

Dashed white lines delineate the graft areas. D: dorsal, V: ventral, M: medial, L: lateral.

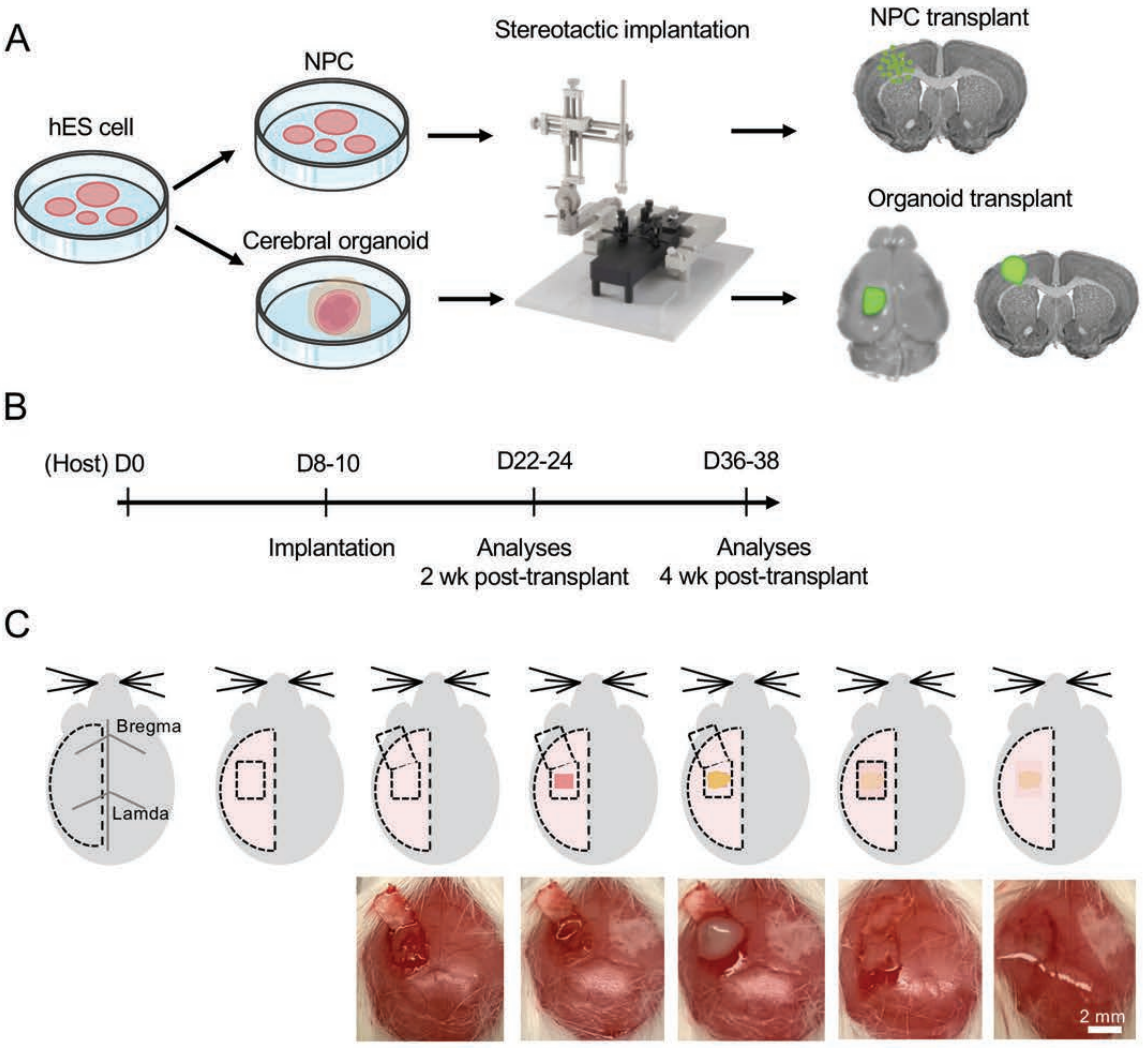

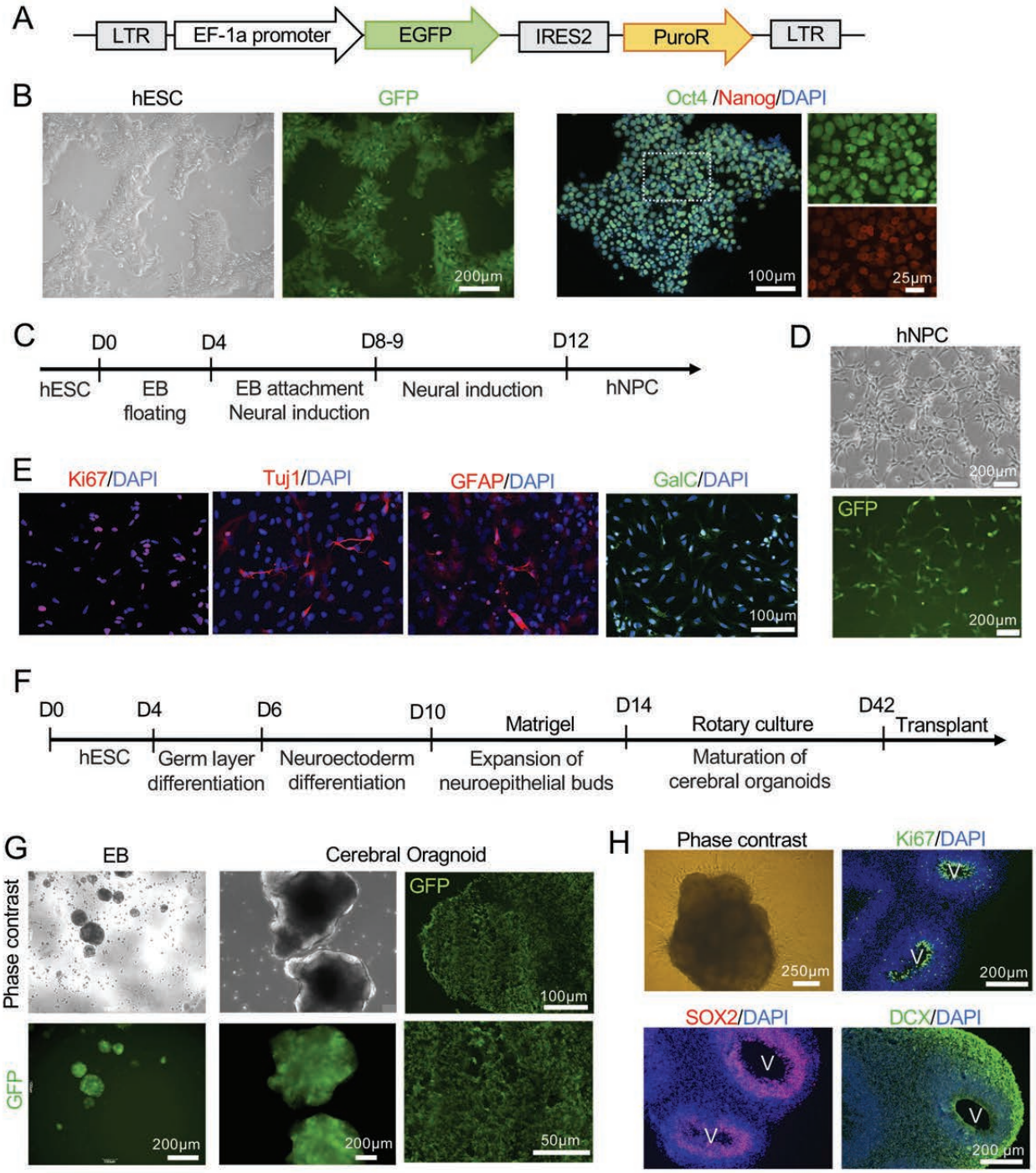

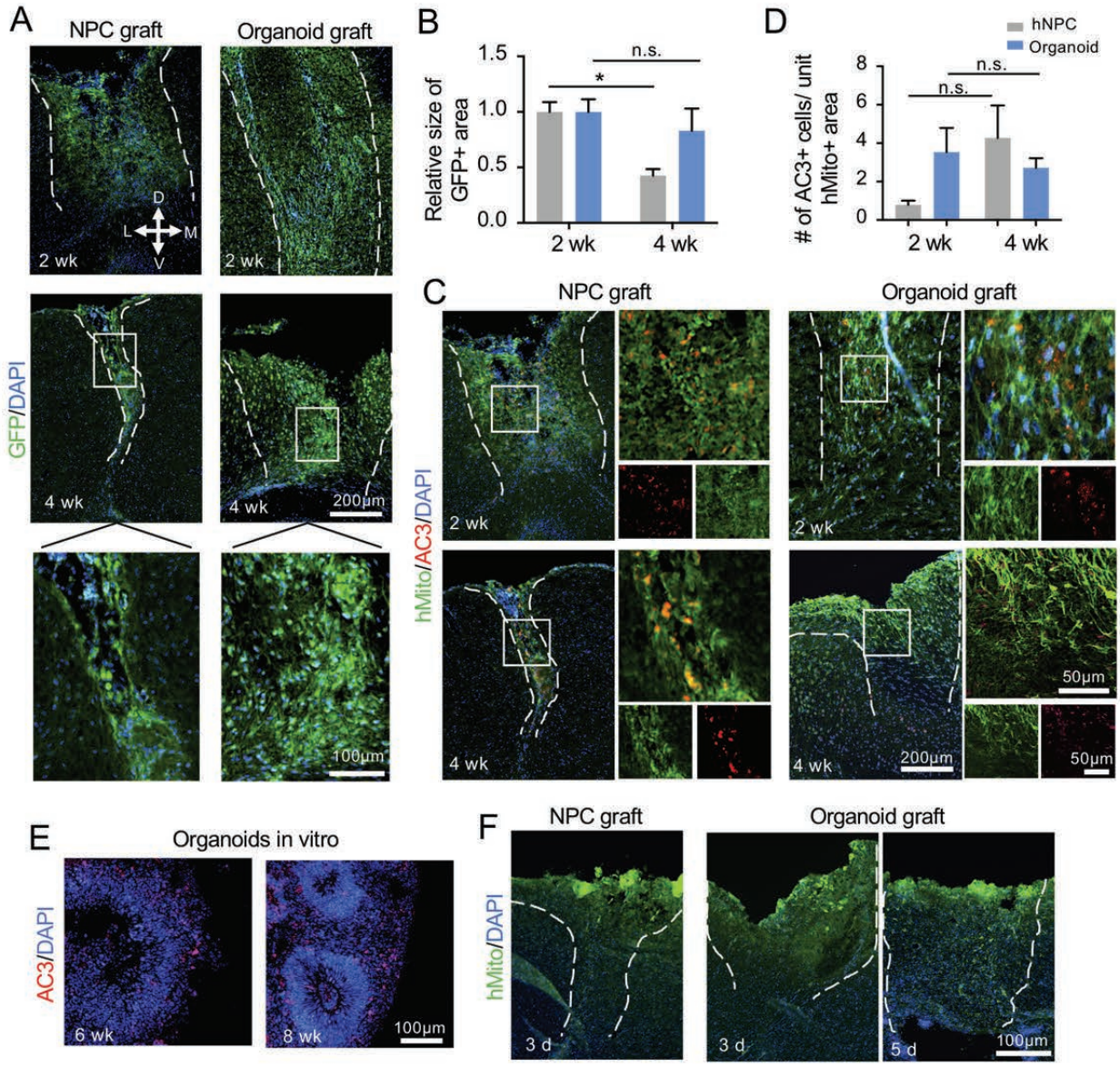

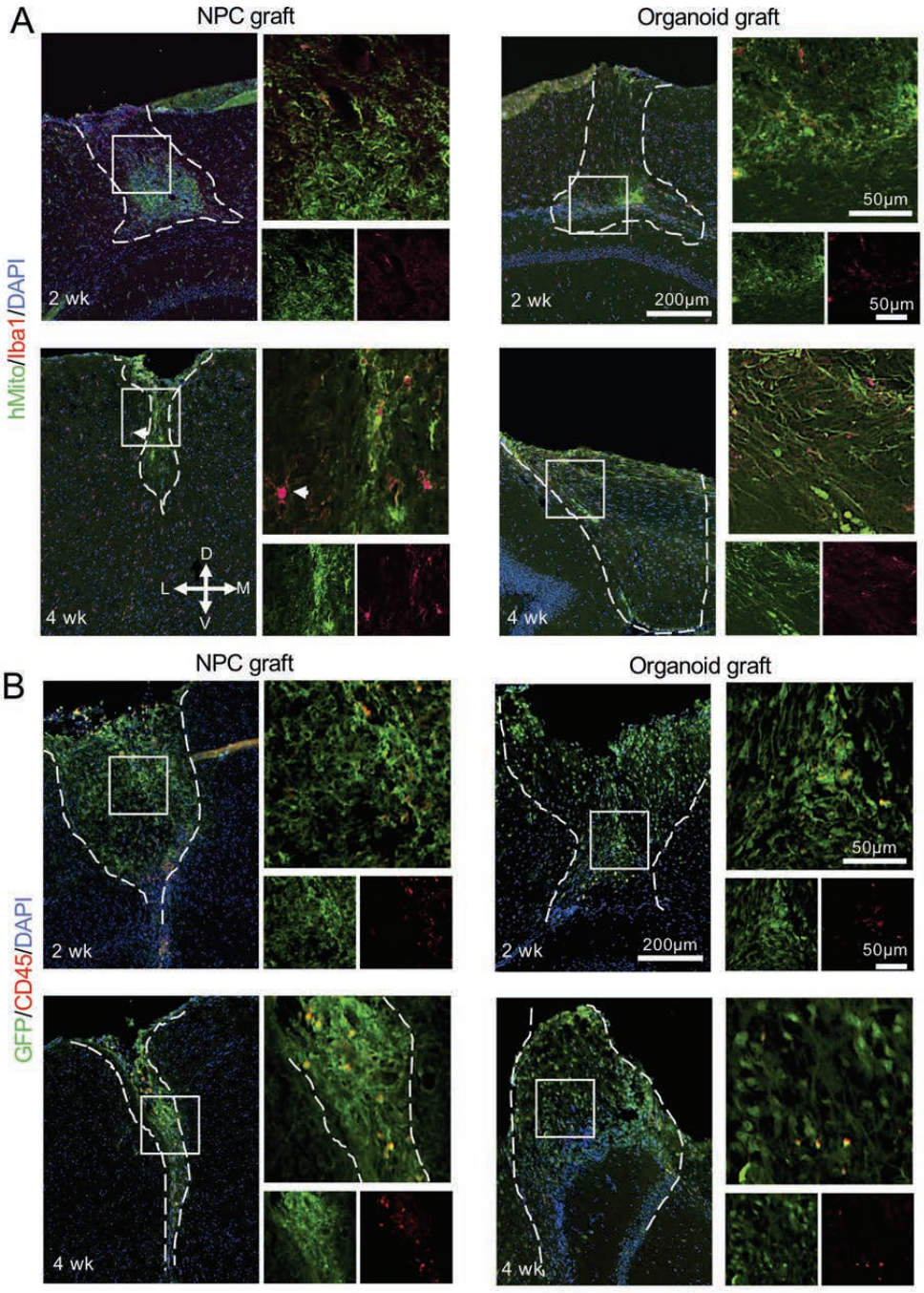

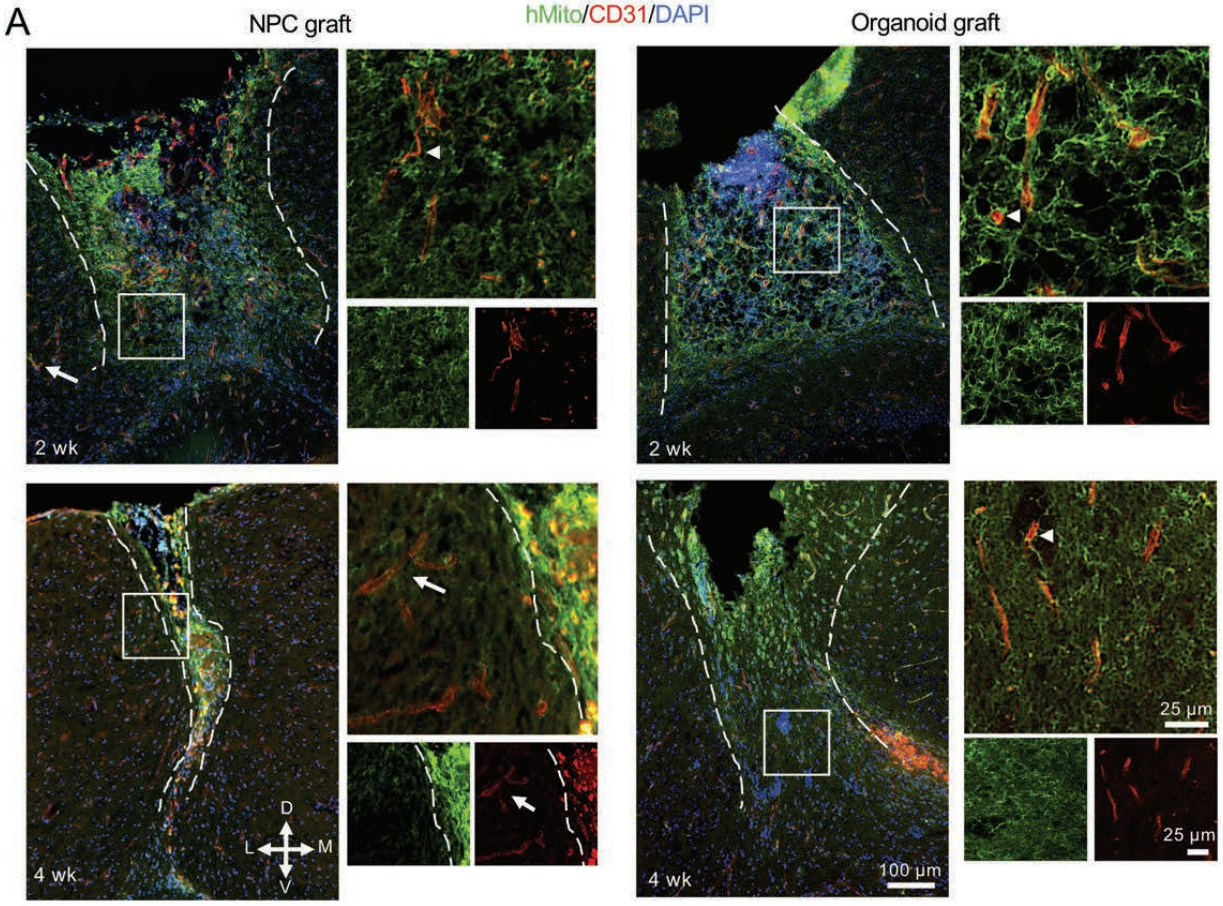

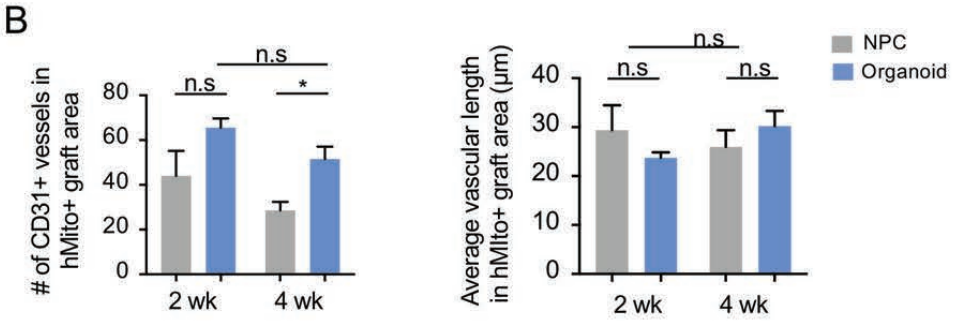

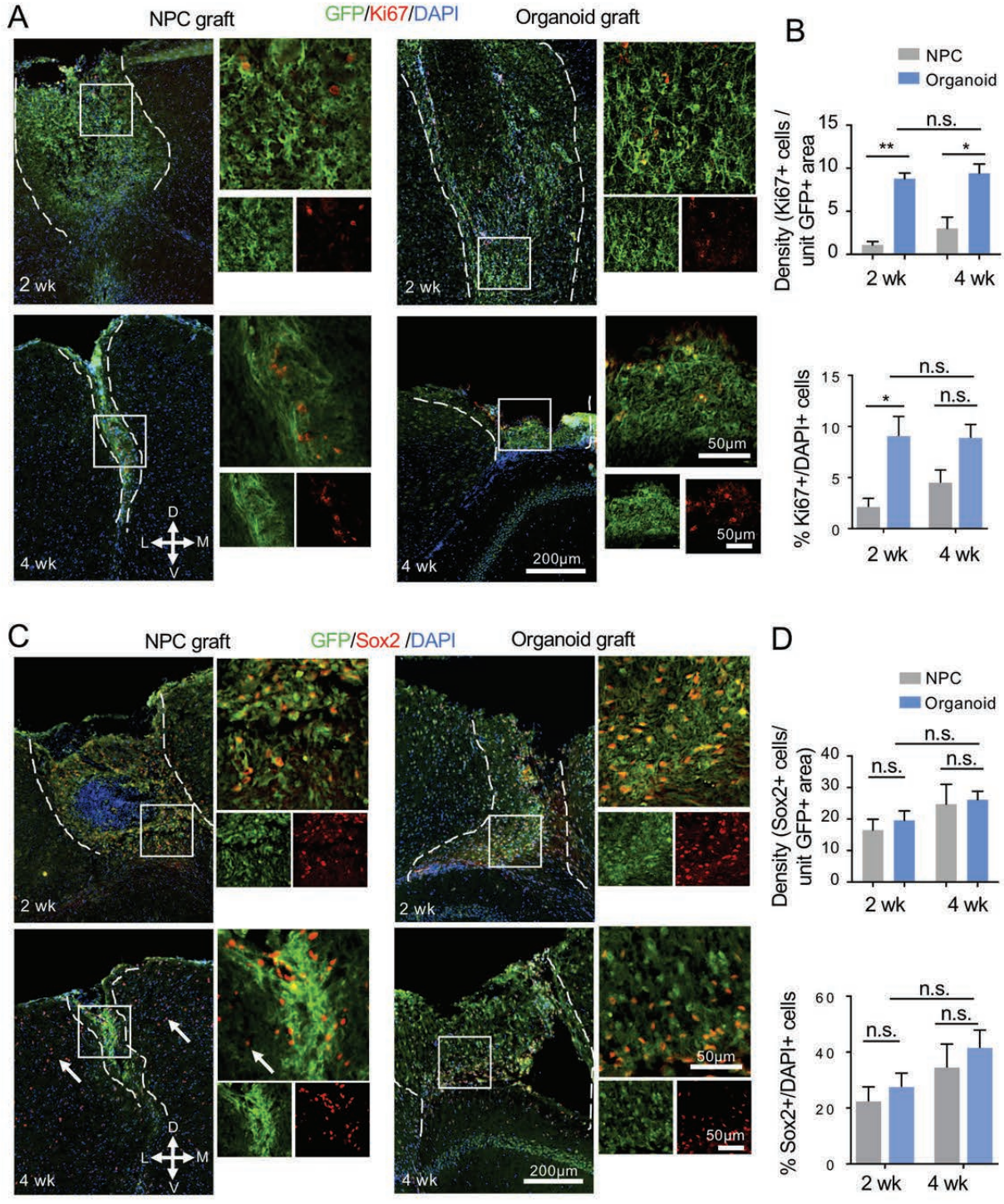

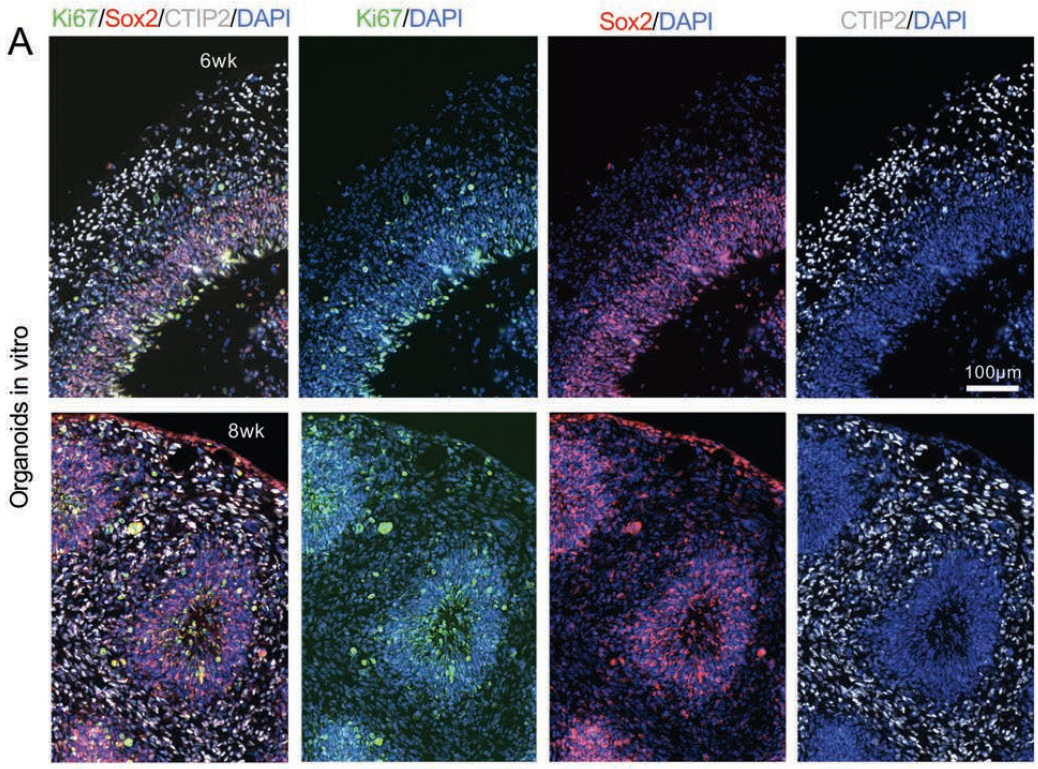

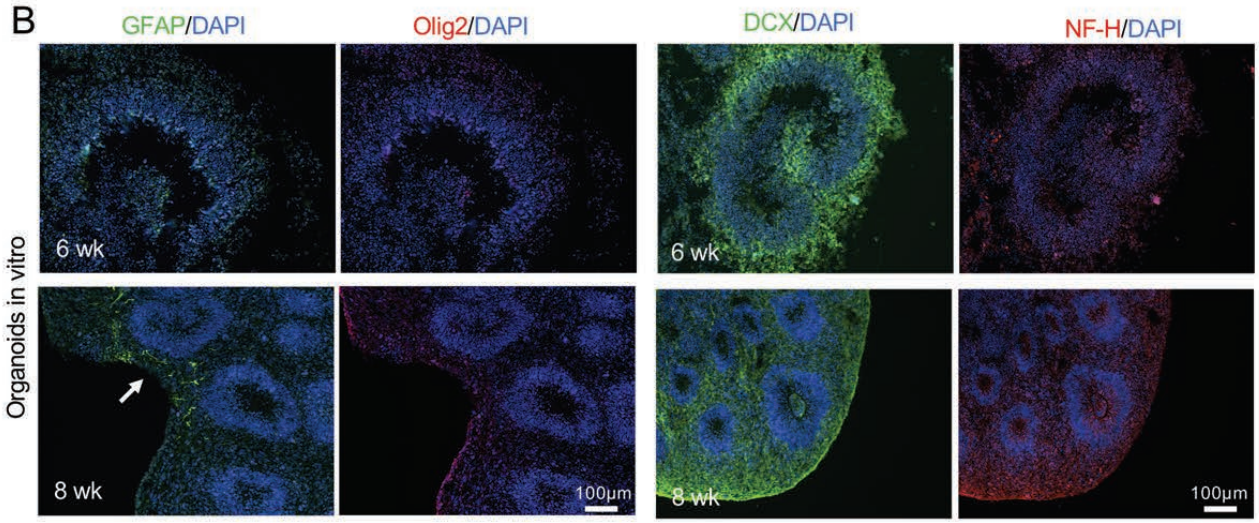

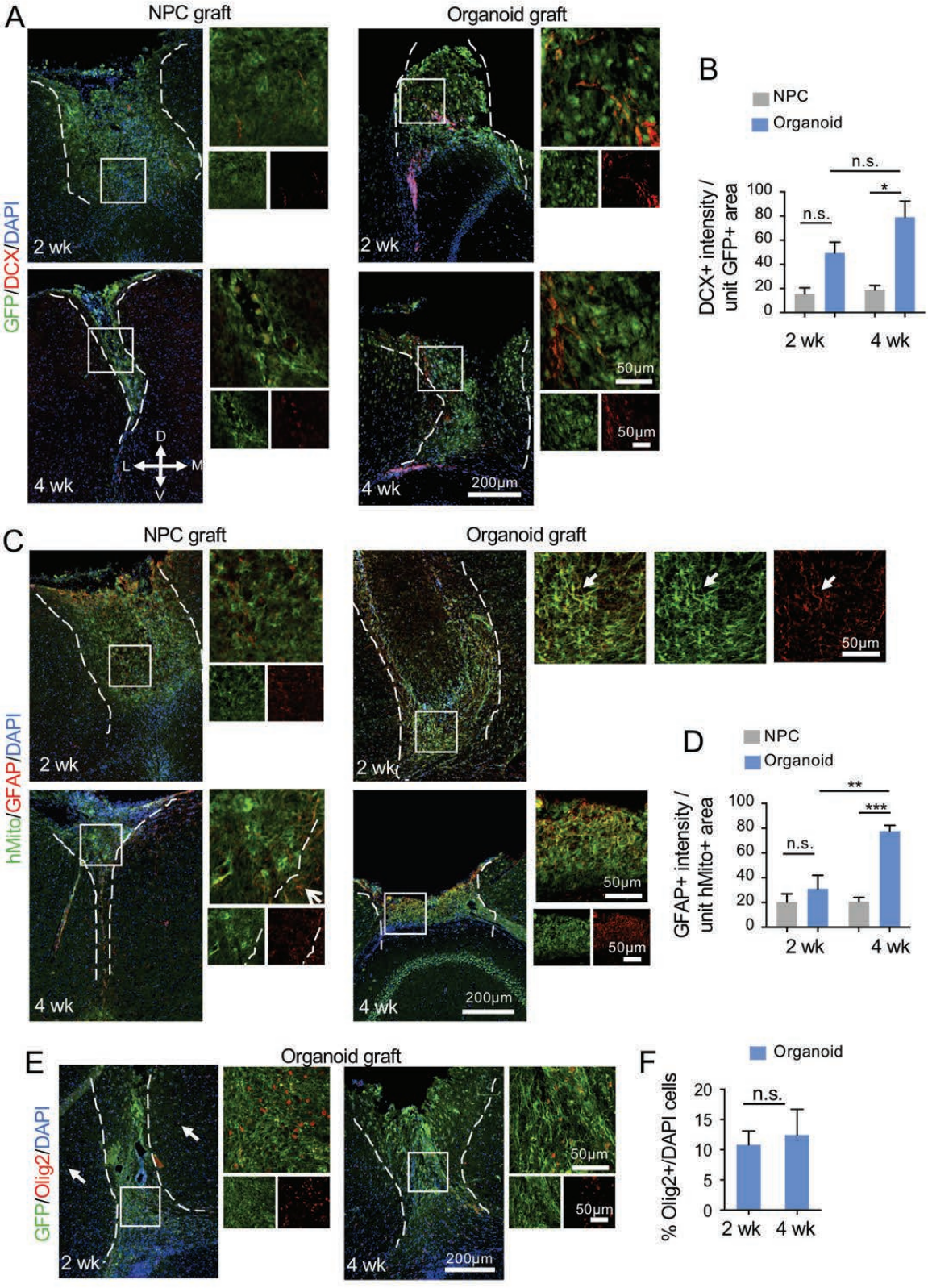

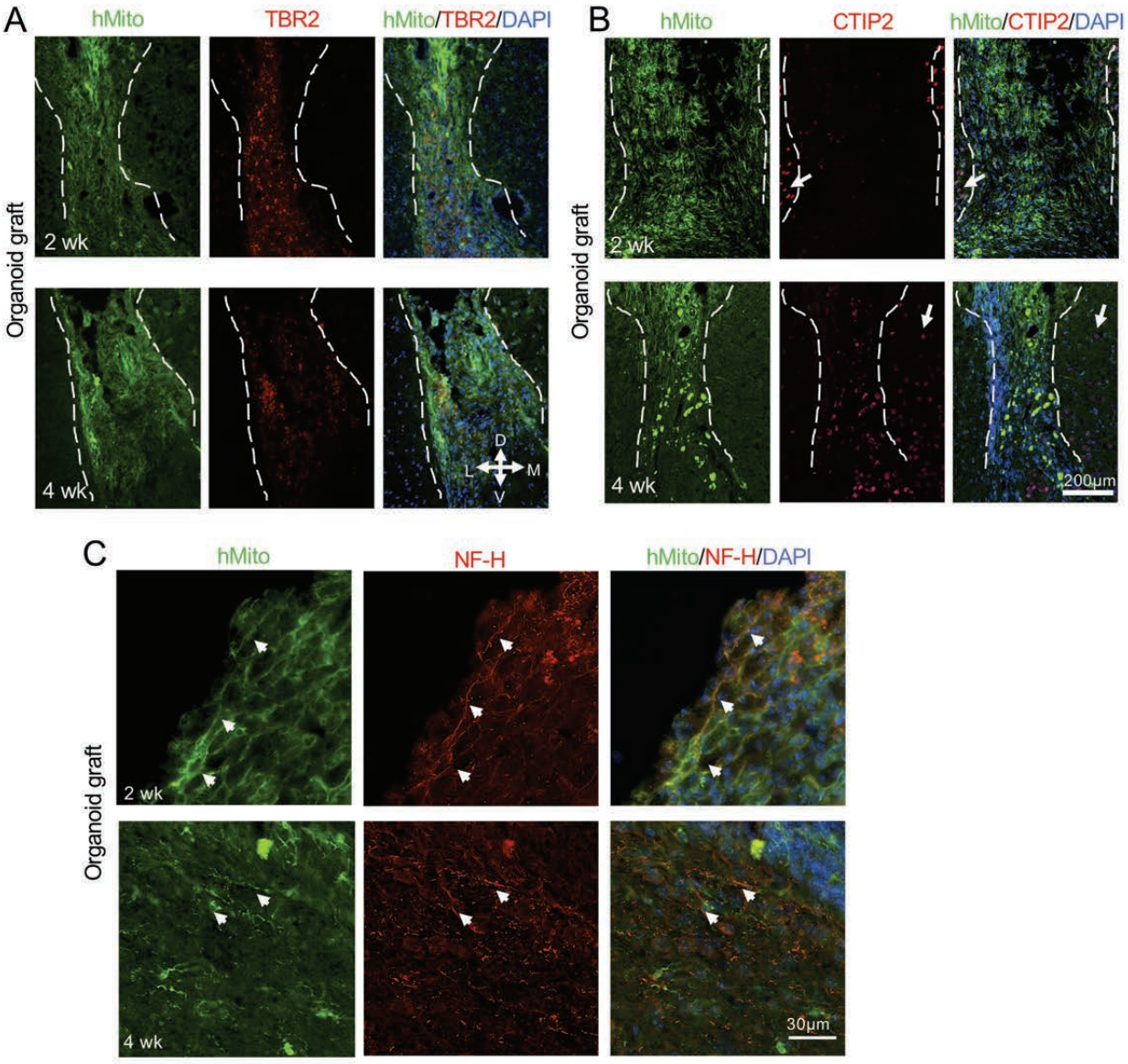

	Data structure	Type of test	Condition	Power

Fig. 3B	Data set with more than 2 groups	Two-way ANOVA - Tukey post-hoc test	2 weeks:Organoids vs. 2 weeks:NPCs	*, p=0.0393
			4 weeks:Organoids vs. 4 weeks:NPCs	n.s., p=0.7729
Fig. 3D	Data set with more than 2 groups	Two-way ANOVA - Tukey post-hoc test	2 weeks:Organoids vs. 2 weeks:NPCs	n.s., p=0.1836
			4 weeks:Organoids vs. 4 weeks:NPCs	n.s., p=0.9634
Fig. 5B - left	Data set with more than 2 groups	Two-way ANOVA - Tukey post-hoc test	2 weeks:Organoids vs. 2 weeks:NPCs	n.s., p=0.1059
			4 weeks:Organoids vs. 4 weeks:NPCs	*, p=0.0293
			4 weeks:Organoids vs. 2 weeks:Organoids	n.s., p=0.4072
Fig. 5B - right	Data set with more than 2 groups	Two-way ANOVA - Tukey post-hoc test	2 weeks:Organoids vs. 2 weeks:NPCs	n.s., p=0.6113
			4 weeks:Organoids vs. 4 weeks:NPCs	n.s., p=0.7485
			4 weeks:Organoids vs. 2 weeks:Organoids	n.s., p=0.2955
Fig. 6B - Top	Data set with more than 2 groups	Two-way ANOVA - Tukey post-hoc test	2 weeks:Organoids vs. 2 weeks:NPCs	**, p=0.0014
			4 weeks:Organoids vs. 4 weeks:NPCs	*, p=0.0108
			4 weeks:Organoids vs. 2 weeks:Organoids	n.s., p=0.9757
Fig. 6B - Bottom	Data set with more than 2 groups	Two-way ANOVA - Tukey post-hoc test	2 weeks:NPC vs. 2 weeks:Organoid	*, p=0.0385
			4 weeks:NPC vs. 4 weeks:Organoid	n.s., p=0.2141
			4 weeks:Organoids vs. 2 weeks:Organoids	n.s., p=0.998
Fig. 6D - Top	Data set with more than 2 groups	Two-way ANOVA - Tukey post-hoc test	2 weeks:Organoids vs. 2 weeks:NPCs	n.s., p= 0.1664
			4 weeks:Organoids vs. 4 weeks:NPCs	n.s., p=0.7125
			4 weeks:Organoids vs. 2 weeks:Organoids	n.s., p=0.3625
Fig. 6D - Bottom	Data set with more than 2 groups	Two-way ANOVA - Tukey post-hoc test	2 weeks:Organoids vs. 2 weeks:NPCs	n.s., p=0.9555
			4 weeks:Organoids vs. 4 weeks:NPCs	n.s., p= 0.9037
			4 weeks:Organoids vs. 2 weeks:Organoids	n.s., p= 0.2857
Fig. 8B	Data set with more than 2 groups	Two-way ANOVA - Tukey post-hoc test	2 weeks:Organoids vs. 2 weeks:NPCs	n.s., p=0.2590
			4 weeks:Organoids vs. 4 weeks:NPCs	*, p=0.0311
			4 weeks:Organoids vs. 2 weeks:Organoids	n.s., p=0.1724
Fig. 8D	Data set with more than 2 groups	Two-way ANOVA - Tukey post-hoc test	2 weeks:Organoids vs. 2 weeks:NPCs	n.s., p=0.6897
			4 weeks:Organoids vs. 4 weeks:NPCs	***, p=0.0006
			4 weeks:Organoids vs. 2 weeks:Organoids	**, p=0.0041
Fig. 8F	Data set with 2 groups	Shapiro-wilk followed by a Student t-test	2 weeks:Organoids vs 4 weeks:Organoids	n.s., p=0.3437

Table 1.